Scientia Africana, Vol. 24 (No. 1), February, 2025. Pp 33-50
© Faculty of Science, University of Port Harcourt, Printed in Nigeria *ISSN 1118 – 1931*

MODELING HEAT TRANSFER TO MAGNETOHYDRODYNAMIC DUSTY FLUID FLOW PAST BETWEEN TWO RIGA PLATES IN A POROUS MEDIUM

Jimoh, O.R., Jatto, A.O. and Yusuf, S.I.
Department of Mathematics, Federal University of Technology, Minna, Nigeria
E-mail: razaq.jimoh@futminna.edu.ng , abdulsamad.jatto@st.futminna.edu.ng , si.yusuf@futminna.edu.ng
Phone: 08077808699, 08130678403, 07069297464

Received: 15-11-2024
Accepted: 30-01-2025

https://dx.doi.org/10.4314/sa.v24i1.4

Journal Homepage: http://www.scientia-african.uniportjournal.info
Publisher: *Faculty of Science, University of Port Harcourt.*

ABSTRACT

In this paper, modeling of an unsteady laminar heat transmittable dusty fluid flow past between two parallel stationary Riga plates is presented. The coupled non-linear partial differential equations governing dusty fluid flow past between two parallel Riga platesin a porous medium were nondimensionalized with the aid of some dimensionless variables and solved analytically using harmonic solution technique. The effects of the various physical parameters on the velocity and temperature of both the fluid and dusty flow were shown graphically and discussed. It is observed that Modified Hartman number increases the velocity of fluid and dusty particles, whereas Grashof number and dimensionless stress coefficient per unit volume decreases the velocity of fluid.

Keywords: MHD fluid, Dusty particle, Riga plate, Porous medium, Magnetic field, Harmonic solution.

INTRODUCTION

The concept of MHD was first introduced by Hannes Alfvén in the 1940s, and since then, it has been extensively studied in various contexts, including astrophysics, geophysics, and engineering. The pioneering work of Pai (1962) and Ferraro (1966) laid the foundation for understanding MHD flows. Later, researchers like. Chiam (1995) and Seddeek (2005) explored MHD flows with dust particles.

The fields of environmental pollution, fluidization, combustion, petroleum, polymer and geophysical procedures, refrigeration, contaminated soil, air, and water, dust or fumes in the gas cooling system, agriculture, crude oil purification, polymer technology and dye systems can all benefit greatly from studies related to the flow and heat transfer of dusty fluids along parallel plates. The Riga plate is made up of permanent magnets and electrodes that associate together to provide a level surface in place of polarity and magnetization. The electromagnetic hydrodynamic fluid behavior is produced by this arrangement, which also reduces pressure and friction (Islam and Nasrin 2020).

Many flow features in contemporary engineering are incomprehensible when using the Newtonian fluid model. Non-Newtonian fluid theory has therefore provided more understandings. Shear stress and shear strain rate have non-linear correlations when the fluid is non-Newtonian. It is widely used in industry and engineering, particularly for the extraction of crude oil from petroleum

products.

Among these fluids is Casson fluid. The most widely used non-Newtonian fluid is called Casson fluid, and it is used in metallurgy, bioengineering, drilling and food processing among other fields (Kataria and Patel 2016).

The research community has been particularly interested in the analysis of flows caused by stretched surfaces in recent years because of their numerous uses in industrial, technical, and biological processes. For instance, the processes involved in crystal growth, polymer extrusion, rubber and plastic sheet manufacture, food processing, glass blowing, and polymer processing, among others. Anjum *et al.* (2018) described the viscous fluid that was thermally stratified and had a stagnation point flow that was dominated by a non-linear, variable-thickness Riga plate. Ahmad (2019) investigated how the Riga plate was affected by the Powell-Eyring and Reiner-Phillipoff fluid flows. What's at stake here are the properties of the nanofluid boundary layer flow within the Riga plate which were also studied by Hayat *et al.* (2016). Iqbal *et al.* (2017) examined a viscous nanofluid with an electrically conductive Riga-plate that could achieve the melting point, thermal radiation and viscous dissipation, andpostulated that the stagnation point flow across the Riga plate has an irregular thickness.

Iqbal *et al.* (2018) also examined the unique outcomes of internal heat generation and thermal deposition on viscous dissipative transport of viscoplastic fluid over a riga-plate. It wasrevealedthat Eckert number, radiation and fluid parameters enhance temperature whereas they contribute in reducingthe rate of heat transfer.

Jimoh and Abdullahi (2023) studied the effect of heat and mass transfer on magneto-hydrodynamic flow with chemical reaction and viscous energy dissipation past an inclined porous plate. Findings from their results revealed that increase in Peclet number; Heat source parameter and Grashof number enhance the velocity profiles.

The unstable free convection Couette flow under the influence of the transverse magnetic field and thermal radiation was examined by Yabo *et al.* (2018). Islam and Nasrin (2021) examined the erratic laminar flow of a dusty, heat-transferable fluid between the two parallel Riga plates. The Riga plates have an impact on the uniform Lorentz forces, and the fluid is subjected to a constant pressure gradient. The lower plate was held stationary while the upper plate moved at a steady speed in accordance with the Couette flow. The Navier-Stokes equation and the Energy equation were both solved using the boundary layer approximations. The implications of the required values on the temperature and velocity distributions as well as the Nusselt number of dust and clean fluid particleswere studied.

Kalpana and Saleem (2022) studied heat transfer of magnetohydrodynamic stratified dusty fluid flow through an inclined irregular porous channel. It was found that the temperature field is higher in the convective boundary than the Navier slip boundary.

Jimoh and Ibrahim (2023) investigated the effect of viscous energy dissipation on transient laminar free convective flow of a dusty viscous fluid through a porous medium. The results obtained revealed that increase in Peclet number, Eckert number and Grashof number leads to increase in the velocity profile. Increase in the mass concentration of the dust particles, concentration resistance ratio, Eckert number and Peclet number leads to increase in the velocity profile of the dust particles. In this research, modeling of an unsteady laminar heat transmittable dusty fluid flow past between two parallel stationary Riga plates is presented and analysed.

Maher*et al.* (2024) explores the effects of dusty fluids with suspended solid particles in a single-walled corrugated channel using electromagnetic hydrodynamics. The analysis of velocity profiles through graphs revealed that corrugation affects fluid and particle velocity behavior, with small amplitude

Scientia Africana, Vol. 24 (No. 1), February, 2025. Pp 33-50
© Faculty of Science, University of Port Harcourt, Printed in Nigeria *ISSN 1118 – 1931*

reducing wave effects and dusty particles boosting velocity.

MODEL FORMULATION

Consider an unsteady incompressible laminar flow of viscous dusty fluid between two horizontal parallel Riga plates embedded in a porous medium. Let both the plates be kept stationary, the lower plate is rest at $\hat{y}$ = −h while the upper plate at $\hat{y}$ = h. The direction of the flow be taken along the x− axis, the $\hat{y}$− axis is perpendicular to the flow and width of the plates parallel to the $\hat{x}\hat{z}$− plane. The fluid is kept in motion by applying a pressure gradient force $\frac{\partial \hat{p}}{\partial \hat{x}}$, also a uniform magnetic force is applied on the fluid, which is influenced by the Riga plate. The velocity components $\hat{v}$ and $\hat{w}$ are zero everywhere at the plate. For dust particle, $\widehat{v_p}$ and $\widehat{w_p}$ are also zero everywhere. Alsoconsider the plate is long enough in x− direction and the fluid motion is two dimensional. But the continuity equation reduces to for the fluid phase $\frac{\partial \hat{u}}{\partial \hat{x}} = 0 \Rightarrow \hat{u} = \hat{u}(\hat{y}, \hat{t})$ and for dust phase $\frac{\partial \widehat{u_p}}{\partial \hat{x}} = 0 \Rightarrow \widehat{u_p} = \widehat{u_p}(\hat{y}, \hat{t})$. The two plates are fixed at two constant temperatures; $\hat{T}_1$ for the lower and $\hat{T}_2$ for the upper plate, where $\hat{T}_2 > \hat{T}_1$. The physical model is shown in figure (1)

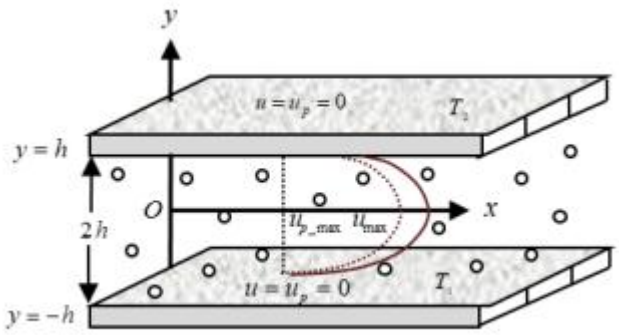

Figure (1)

Due the Riga plate, the Lorentz force $\bar{f} = \hat{J}\Lambda\hat{B} \approx \sigma(\hat{E}\Lambda\hat{B})$ is defined as magnetic force. According to the Grinberg hypothesis this magnetic force is defined as follows$\bar{f} = \hat{J}\Lambda\hat{B} = \left(\frac{\pi}{8\rho}J_0M_0e^{-\frac{\pi}{l}y}, 0, \frac{\pi}{8\rho}J_0M_0e^{-\frac{\pi}{l}y}\right)$.

In view of Islam and Nasrin (2020) under the consideration of above assumptions, and also applying Boussinesq approximation on the fluid, the dimensional forms of the momentum and energy equations for the clean fluid and the dust particle are expressed as follows:

Momentum equation for fluid phase

$$\frac{\partial \hat{u}}{\partial \hat{t}} = -\frac{1}{\rho}\frac{\partial \hat{p}}{\partial \hat{x}} + \frac{v\partial^2\hat{u}}{\partial \hat{y}^2} + \frac{\pi}{8\rho}J_0M_0e^{-\frac{\pi}{l}y} - \frac{1}{\rho}KN\left(\hat{u} - \widehat{u_p}\right) - \frac{v}{k}\hat{u} - \frac{\sigma_eB_0^2}{\rho}\hat{u} + g\beta(\hat{T} - \hat{T}_2) \qquad (1)$$

Momentum equation for dusty phase

$$m_p\frac{\partial \widehat{u_p}}{\partial \hat{t}} = \mu_p\frac{\partial^2\widehat{u_p}}{\partial \hat{y}^2} + KN\left(\hat{u} - \widehat{u_p}\right) \qquad (2)$$

Energy equation for fluid phase

$$\frac{\partial \hat{T}}{\partial \hat{t}} = \frac{k}{\rho c_p}\frac{\partial^2\hat{T}}{\partial \hat{y}^2} - \frac{2kKN}{3\rho^2c_pv}\left(\hat{T} - \widehat{T_p}\right) + \frac{v}{c_p}\left(\frac{\partial \hat{u}}{\partial \hat{y}}\right)^2 - \frac{1}{\rho c_p}\frac{\partial \hat{q}}{\partial \hat{y}} \qquad (3)$$

Energy equation for dusty phase

$$\frac{\partial \widehat{T_p}}{\partial \hat{t}} = \frac{k}{\rho c_p}\frac{\partial^2 \widehat{T_p}}{\partial \hat{y}^2} + \frac{1}{\gamma_T}\left(\hat{T} - \widehat{T_p}\right) \quad (4)$$

Initial and boundary condition

$$\hat{u} = 0, \hat{u}_p = 0, \hat{T} = \hat{T}_1, \hat{T}_p = \hat{T}_1 at \hat{y} = -h \quad (5)$$

$$\hat{u} = 0, \hat{u}_p = 0, \hat{T} = \hat{T}_2, \hat{T}_p = \hat{T}_2 at \hat{y} = h$$

Non-Dimensionlization

Equation (1) to (4) are non-dimensionalized using the following dimensionless variable

$$x = \frac{\pi}{l}\hat{x}, y = \frac{\pi}{l}\hat{y}, u = \frac{l}{\pi v}\hat{u}, u_p = \frac{l}{\pi v}\widehat{u_p}, p = \frac{l^2\hat{p}}{\pi^2\rho v^2}, t = \frac{\pi^2 v\hat{t}}{l^2}, \theta = \frac{\hat{T}-\hat{T}_1}{\hat{T}_2-\hat{T}_1}, \theta_p = \frac{\hat{T}_p-\hat{T}_1}{\hat{T}_2-\hat{T}_1} \quad (6)$$

Now

$$\partial\hat{x} = \frac{l}{\pi}\partial x, \partial\hat{y} = \frac{l}{\pi}\partial y, \partial\hat{u} = \frac{\pi v}{l}\partial u, \partial\widehat{u_p} = \frac{\pi v}{l}\partial u_p, \partial\hat{p} = \frac{\pi^2\rho v^2}{l^2}\partial p, \partial\hat{t} = \frac{l^2}{\pi^2 v}\partial t, \quad (7)$$

$$\widehat{\partial T} = \left(\hat{T}_2-\hat{T}_1\right)\partial\theta, \widehat{\partial T_p} = \left(\hat{T}_2-\hat{T}_1\right)\partial\theta_p$$

Substitute equation (7) into equation (1) and simplifying, the following equation is obtained

$$\frac{\pi^3 v^2}{l^3}\frac{\partial u}{\partial t} = -\frac{\pi^3 v^2}{l^3}\frac{\partial p}{\partial x} + \frac{\pi^3 v^2}{l^3}\frac{\partial^2 u}{\partial y^2} + \frac{\pi}{8\rho}J_0 M_0 e^{-y} - \frac{1}{\rho}KN\left(\frac{\pi v}{l}\right)\left(u - u_p\right) - \frac{v^2}{k}\frac{\pi}{l}u - \frac{\sigma_e B_0^2}{\rho}\frac{\pi v}{l}u + g\beta\left(\left(\left(\widehat{T_2} - \hat{T}_1\right)\theta + \hat{T}_1\right) - \hat{T}_2\right) \quad (8)$$

Multiply through by $\frac{l^3}{\pi^3 v^2}$

$$\frac{\partial u}{\partial t} = -\frac{\partial p}{\partial x} + \frac{\partial^2 u}{\partial y^2} + \frac{l^3 J_0 M_0}{\pi^2 v^2 8\rho}e^{-y} - \frac{KNl^2}{\rho v\pi^2}\left(u - u_p\right) - \frac{l^2}{\pi^2 k}u - \frac{\sigma_e B_0^2 l^3}{\rho\pi^2 v}u + \frac{g\beta l^3\left(\left(\widehat{T_2}-\hat{T}_1\right)(\theta-1)\right)}{\pi^3 v^2} \quad (9)$$

Equation (9) becomes

$$\frac{\partial u}{\partial t} = \alpha + \frac{\partial^2 u}{\partial y^2} + H_r e^{-y} - R\left(u - u_p\right) - \frac{u}{K} - \frac{\sigma_e B_0^2 l^3}{\rho\pi^2 v}u + G_r(\theta - 1) \quad (10)$$

Substitute equation (7) into equation (2) and simplifying, the following equation is obtained

$$m_p\frac{\pi^3 v^2}{l^3}\frac{\partial u_p}{\partial t} = \mu_p\frac{\pi^3 v^2}{l^3}\frac{\partial^2 u}{\partial y^2} + KN\left(\frac{\pi v}{l}\right)\left(u_p - u\right) \quad (11)$$

Multiply through by $\frac{l^3}{m_p\pi^3 v^2}$

$$\frac{\partial u_p}{\partial t} = \frac{\mu_p}{m_p}\frac{\partial^2 u}{\partial y^2} + \frac{KNl^2}{m_p v\pi^2}\left(u_p - u\right) \quad (12)$$

$$\frac{\partial u_p}{\partial t} = \beta\frac{\partial^2 u}{\partial y^2} + \frac{1}{G}\left(u - u_p\right) \quad (13)$$

The fluid is assumed to be optically thin with a relatively low density and radiative heat flux as given by Cogley *et al.* (1968).

$$\frac{\partial\hat{q}}{\partial\hat{y}} = 4\alpha^2\left(\hat{T}_2 - \hat{T}\right) \quad (14)$$

Substitute equation (7) into equation (3) and simplifying, the following equation is obtained

Scientia Africana, Vol. 24 (No. 1), February, 2025. Pp 33-50
© Faculty of Science, University of Port Harcourt, Printed in Nigeria *ISSN 1118 – 1931*

$$\frac{(\hat{T}_2-\hat{T}_1)\partial\theta}{\frac{l^2}{\pi^2 v}\partial t}=\frac{k}{\rho c_p}\frac{\partial(\hat{T}_2-\hat{T}_1)\partial\theta}{\left(\frac{l}{\pi}\right)^2\partial y^2}-\frac{2kKN}{3\rho^2 c_p v}\left(\left(\left(\left(\hat{T}_2-\hat{T}_1\right)\theta+\hat{T}_1\right)\right)-\left(\left(\hat{T}_2-\hat{T}_1\right)\theta_p+\hat{T}_1\right)\right)+$$

$$\frac{v}{c_p}\left(\frac{\frac{\pi v}{l}}{\frac{l}{\pi}}\right)^2\left(\frac{\partial u}{\partial y}\right)^2-\frac{1}{\rho c_p}4\alpha^2\left(\hat{T}_2-\left(\left(\hat{T}_2-\hat{T}_1\right)\theta+\hat{T}_1\right)\right) \quad (15)$$

Multiply through by $\frac{l^2}{(\hat{T}_2-\hat{T}_1)\pi^2 v}$

$$\frac{\partial\theta}{\partial t}=\frac{k}{\rho v c_p}\frac{\partial^2\theta}{\partial y^2}-\frac{2kKNl^2}{3\rho^2 c_p v\pi^2 v}\left(\theta-\theta_p\right)+\frac{v\pi^2 v}{c_p l^2(\hat{T}_2-\hat{T}_1)}\left(\frac{\partial u}{\partial y}\right)^2-\frac{l^2}{\rho\pi^2 v c_p}4\alpha^2(1-\theta) \quad (16)$$

$$\frac{\partial\theta}{\partial t}=\frac{1}{P_r}\frac{\partial^2\theta}{\partial y^2}-\frac{2R}{3P_r}\left(\theta-\theta_p\right)+E_c\left(\frac{\partial u}{\partial y}\right)^2-N_r(1-\theta) \quad (17)$$

Substitute equation (7) into equation (4) and simplifying, the following equation is obtained

$$\frac{(\hat{T}_2-\hat{T}_1)\partial\theta_p}{\frac{l^2}{\pi^2 v}\partial t}=\frac{k}{\rho c_p}\frac{\partial(\hat{T}_2-\hat{T}_1)\partial\theta_p}{\left(\frac{l}{\pi}\right)^2\partial y^2}+\frac{1}{\gamma_T}\left(\left(\left(\left(\hat{T}_2-\hat{T}_1\right)\theta+\hat{T}_1\right)\right)-\left(\left(\hat{T}_2-\hat{T}_1\right)\theta_p+\hat{T}_1\right)\right) \quad (18)$$

Multiply through by $\frac{l^2}{(\hat{T}_2-\hat{T}_1)\pi^2 v}$

$$\frac{\partial\theta_p}{\partial t}=\frac{k}{\rho c_p v}\frac{\partial^2\theta_p}{\partial y^2}+\frac{l^2}{\pi^2 v\gamma_T}\left(\theta-\theta_p\right) \quad (19)$$

$$\frac{\partial\theta_p}{\partial t}=\frac{1}{P_r}\frac{\partial^2\theta_p}{\partial y^2}+L_0\left(\theta-\theta_p\right) \quad (20)$$

From equation (10)

$$\frac{\partial u}{\partial t}=\alpha+\frac{\partial^2 u}{\partial y^2}+H_r e^{-y}-\left(R+\frac{1}{K}+H\right)u+Ru_p+G_r(\theta-1) \quad (21)$$

$$\frac{\partial u}{\partial t}=\alpha+\frac{\partial^2 u}{\partial y^2}+H_r e^{-y}-\varepsilon u+Ru_p+G_r(\theta-1) \quad (22)$$

Where: $\varepsilon=\left(R+\frac{1}{K}+H\right)$ and $H=\frac{\sigma_e B_0^2 l^3}{\rho\pi^2 v}$ (23)

Also from equation (13)

$$\frac{\partial u_p}{\partial t}=\beta\frac{\partial^2 u}{\partial y^2}+\frac{1}{G}\left(u-u_p\right) \quad (24)$$

For the energy equation (17)

$$\frac{\partial\theta}{\partial t}=\frac{1}{P_r}\frac{\partial^2\theta}{\partial y^2}-\frac{2R}{3P_r}\theta+\frac{2R}{3P_r}\theta_p+E_c\left(\frac{\partial u}{\partial y}\right)^2+N_r\theta-N_r \quad (25)$$

$$\frac{\partial\theta}{\partial t}=\frac{1}{P_r}\frac{\partial^2\theta}{\partial y^2}-\left(\frac{2R}{3P_r}-N_r\right)\theta+\frac{2R}{3P_r}\theta_p-N_r+E_c\left(\frac{\partial u}{\partial y}\right)^2 \quad (26)$$

$$\frac{\partial\theta}{\partial t}=\frac{1}{P_r}\frac{\partial^2\theta}{\partial y^2}-B_3\theta+B_2\theta_p-N_r+E_c\left(\frac{\partial u}{\partial y}\right)^2 \quad (27)$$

Also

$$\frac{\partial\theta_p}{\partial t}=\frac{1}{P_r}\frac{\partial^2\theta_p}{\partial y^2}-L_0\theta_p+L_0\theta \quad (28)$$

The dimensionless equations are

Momentum equations:

Fluid phase

$$\frac{\partial u}{\partial t} = \alpha + \frac{\partial^2 u}{\partial y^2} + H_r e^{-y} - \varepsilon u + R u_p + G_r(\theta - 1) \tag{29}$$

Dusty phase

$$\frac{\partial u_p}{\partial t} = \beta \frac{\partial^2 u}{\partial y^2} + \frac{1}{G}\left(u_p - u\right) \tag{30}$$

Energy equations:

Fluid phase

$$\frac{\partial \theta}{\partial t} = \frac{1}{P_r}\frac{\partial^2 \theta}{\partial y^2} - B_3\theta + B_2\theta_p - N_r + E_c\left(\frac{\partial u}{\partial y}\right)^2 \tag{31}$$

Dusty phase

$$\frac{\partial \theta_p}{\partial t} = \frac{1}{P_r}\frac{\partial^2 \theta_p}{\partial y^2} - L_0\theta_p + L_0\theta \tag{32}$$

Where:

$\alpha = -\frac{\partial p}{\partial x}$ (dimensionless pressure gradient)

$H_r = \frac{l^3 J_0 M_0}{\pi^2 v^2 8\rho}$ (modified Hartman number)

$R = \frac{KNl^2}{\rho v \pi^2}$ (fluid concentration parameter)

$G = \frac{m_p v \pi^2}{Kl^2}$ (particle mass parameter)

$\beta = \frac{\mu_p}{m_p v}$ (dimensionless stress coefficient per unit volume)

$P_r = \frac{\rho v c_p}{k}$ (Prandtl number)

$E_c = \frac{v^2\pi^2}{c_p l^2(\widehat{T_2} - \widehat{T_1})}$ (Eckert number)

$L_0 = \frac{l^2}{\pi^2 v \gamma_T}$ (temperature relaxation time parameter)

$N_r = \frac{l^2}{\rho \pi^2 v c_p} 4\alpha^2$ (radiation parameter)

$G_r = \frac{g\beta l^3(\widehat{T_2} - \widehat{T_1})}{\pi^3 v^2}$ (Grashof number)

$K = \frac{\pi^2 k}{l^2}$ (stoke constant)

$H = \frac{\sigma_e B_0^2 l^3}{\rho \pi^2 v}$ (Hartman number)

$B_3 = B_2 - N_r$ and $B_2 = \frac{2R}{3P_r}$

Scientia Africana, Vol. 24 (No. 1), February, 2025. Pp 33-50
© Faculty of Science, University of Port Harcourt, Printed in Nigeria *ISSN 1118 – 1931*

Equation (29) to equation (32) are subject to the initial and boundary conditions:

$$\left.\begin{aligned} u = 0, u_p = 0, \theta = 0, \theta_p = 0 \;\; aty = -h \\ u = 0, u_p = 0, , \theta = 1, \theta_p = 1 \;\; aty = h \end{aligned}\right\} \quad (33)$$

MATERIALS AND METHODS

For any oscillatory flow, we assume

$$\alpha = -\frac{\partial p}{\partial x} = \sigma e^{iwt}, u(y,t) = u(y)e^{iwt}, \theta(y,t) = \theta(y)e^{2iwt}, \quad (34)$$

$$u_p(y,t) = u_p(y)e^{iwt}, \theta_p(y,t) = \theta_p(y)e^{2iwt} \quad \text{(Mehta } et\ al.\text{, 2020)}$$

By substituting equation (34) in equations (29), (30), (31) and (32), the following equations are obtained:

$$\frac{d^2u}{dy^2} - \lambda_1^2 u = -\left(Ru_p + G_r e^{iwt}\theta - G_r e^{-iwt} + \sigma + H_r e^{-(iwt+y)}\right) \quad (35)$$

$$\frac{d^2u_p}{dy^2} - \lambda_2^2 u_p = -\frac{1}{\beta G}u \quad (36)$$

$$\frac{d^2\theta}{dy^2} - \lambda_3^2 \theta = -B_2 P_r \theta_p - P_r E_c \left(\frac{du(y)}{dy}\right)^2 + P_r N_r e^{-2iwt} \quad (37)$$

$$\frac{d^2\theta_p}{dy^2} - \lambda_4^2 \theta_p = -P_r L_0 \theta \quad (38)$$

Where:

$$\left.\begin{aligned} \lambda_1^2 &= \varepsilon + iw \\ \lambda_2^2 &= \frac{iw + \frac{1}{G}}{\beta} \\ \lambda_3^2 &= P_r B_3 + 2iwP_r \\ \lambda_4^2 &= P_r(2iw + L_0) \end{aligned}\right\} \quad (39)$$

The boundary conditions are transformed in line with fully oscillatory flow conditions as follows

$$\left.\begin{aligned} u(-h) = \frac{0}{e^{iwt}} = 0, u(h) = \frac{0}{e^{iwt}} = 0 \\ u_p(-h) = \frac{0}{e^{iwt}} = 0, u_p(h) = \frac{0}{e^{iwt}} = 0 \\ \theta(-h) = \frac{0}{e^{2iwt}} = 0, \theta(h) = \frac{1}{e^{2iwt}} = e^{-2iwt} \\ \theta_p(-h) = \frac{0}{e^{2iwt}} = 0, \theta_p(h) = \frac{1}{e^{2iwt}} = e^{-2iwt} \end{aligned}\right\} \quad (40)$$

Therefore, the boundary conditions are,

$$\left.\begin{aligned} u(-1) = 0, u(1) = 0 \\ u_p(-1) = 0, u_p(1) = 0 \\ \theta(-1) = 0, \theta(1) = e^{-2iwt} \\ \theta_p(-1) = 0, \theta_p(1) = e^{-2iwt} \end{aligned}\right\} \quad (41)$$

Let

0< Gr << 1 such that

$$\left.\begin{aligned} &\text{R = aGr, } \frac{1}{G} = \text{b Gr, Pr = dGr} \\ &\text{Now } u(y) = u_0(y) + G_r u_1(y) + \cdots \\ &u_p(y) = u_{p0}(y) + G_r u_{p1}(y) + \cdots \\ &\theta(y) = \theta_0(y) + G_r \theta_1(y) + \cdots \\ &\theta_p(y) = \theta_{p0}(y) + G_r \theta_{p1}(y) + \cdots \end{aligned}\right\} \quad (42)$$

Therefore

$$\left.\begin{aligned} u_0(-1) = 0, u_0(1) = 0, u_1(-1) = 0, u_1(1) = 0 \\ u\_p0\ (-1) = 0, u\_p0\ (1) = 0, u\_p1\ (-1) = 0, u\_p1\ (1) = 0 \\ \theta_0(-1) = 0, \theta_0(1) = e^{-2iwt}, \theta_1(-1) = 0, \theta_1(1) = 0 \\ \theta_{p0}(-1) = 0, \theta_{p0}(1) = e^{-2iwt}, \theta_{p1}(-1) = 0, \theta_{p1}(1) = 0 \end{aligned}\right\} \quad (43)$$

By substituting equation (42) in equation (35) and equating coefficients of corresponding terms on both sides, the following set of equations are obtained:

For order 0,$G_r{}^0$: 1

$$\frac{\mathrm{d}^2 u_O}{\mathrm{d}y^2} - \lambda_1^2 u_0 = -(\sigma + Hre^{-(iwt + y)}) \quad (44)$$

$$u_0(-1) = 0, u_0(1) = 0$$

For order 1,$G_r{}^1$: G_r

$$\frac{\mathrm{d}^2 u_1}{\mathrm{d}y^2} - \lambda_1^2 u_1 = -\left(a u_{p0} + e^{iwt}\theta_0 - e^{iwt}\right) \quad (45)$$

$$u_1(-1) = 0, u_1(1) = 0$$

By substituting equation (42) in equation (36) and equating coefficients of corresponding terms on both sides, the following set of equations are obtained:

For order 0,$G_r{}^0$: 1

$$\frac{\mathrm{d}^2 u_{P0}}{\mathrm{d}y^2} - \lambda_2^2 u_{p0} = 0 \quad (46)$$

$$u_{p0}(-1) = 0, u_{p0}(1) = 0$$

For order 1,$G_r{}^1$: G_r

$$\frac{\mathrm{d}^2 u_{p1}}{\mathrm{d}y^2} - \lambda_2^2 u_{p1} = -\frac{b}{\beta} u_o \quad (47)$$

$$u_{p1}(-1) = 0, u_{p1}(1) = 0$$

By substituting equation (42) in equation (37) and equating coefficients of corresponding terms on both sides, the following set of equations are obtained:

For order 0,$G_r{}^0$: 1

Scientia Africana, Vol. 24 (No. 1), February, 2025. Pp 33-50
© Faculty of Science, University of Port Harcourt, Printed in Nigeria *ISSN 1118 – 1931*

$$\frac{\mathrm{d}^2\theta_o}{\mathrm{d}y^2} - \lambda_3^2\theta_O = 0 \quad (48)$$

$\theta_0(-1) = 0, \theta_0(1) = e^{-2iwt}$

For order 1,$G_r{}^1$: G_r

$$\frac{\mathrm{d}^2\theta_1}{\mathrm{d}y^2} - \lambda_3^2\theta_1 = -B_2 d\theta p_o - dEc\left(\frac{du_o}{dy}\right)^2 - dNre^{-2iwt} \quad (49)$$

$\theta_1(-1) = 0, \theta_1(1) = 0$

By substituting equation (42) in equation (38) and equating coefficients of corresponding terms on both sides, the following set of equations are obtained:

For order 0,$G_r{}^0$: 1

$$\frac{\mathrm{d}^2\theta p_o}{\mathrm{d}y^2} - \lambda_4^2\theta p_o = 0 \quad (50)$$

$\theta_{p0}(-1) = 0, \theta_{p0}(1) = e^{-2iwt}$,

For order 1,$G_r{}^1$: G_r

$$\frac{\mathrm{d}^2\theta p_1}{\mathrm{d}y^2} - \lambda_4^2\theta p_1 = -dLo\theta_o \quad (51)$$

$\theta_{p1}(-1) = 0, \theta_{p1}(1) = 0$

The boundary value problems (44) to (51) are solved by the method of undetermined coefficients and obtained the following results:

$$u(y,t) = \left[A_7 e^{\lambda_1 y} + A_6 e^{-\lambda_1 y} + A_5 e^{-y} + A_4 + G_r\left(A_{22}e^{\lambda_1 y} + A_{21}e^{-\lambda_1 y} + A_{18e^{\lambda_3 y}} + A_{19e^{-\lambda_3 y}} + A_{20}\right)\right]e^{iwt} \quad (52)$$

$$u_p(y,t) = \left[G_r\left(A_{17}\, e^{\lambda_2 y} + A_{16}\, e^{-\lambda_2 y} + A_{12}\, e^{\lambda_1 y} + A_{14}\, e^{-y} + A_{15}\right)\right]e^{iwt} \quad (53)$$

$$\theta(y,t) = \left[A_3\, e^{\lambda_3 y} + A_2\, e^{-\lambda_3 y} + G_r\left(A_{32}e^{\lambda_3 y} + A_{31}e^{-\lambda_3 y} + A_{23}e^{\lambda_4 y} + A_{24}e^{-\lambda_4 y} + A_{25}e^{2\lambda_1 y} + A_{26}e^{(\lambda_1 - 1)y} + A_{27}e^{(-\lambda_1 - 1)y} + A_{28}e^{-2\lambda_1 y} + A_{29}e^{-2y} + A_{30}\right)\right]e^{2iwt} \quad (54)$$

$$\theta_p(y,t) = \begin{bmatrix} A_1 e^{\lambda_4 y} + A_0 e^{-\lambda_4 y} + \\ G_r\left(A_{11}e^{\lambda_4 y} + A_{10}e^{-\lambda_4 y} + A_8 e^{\lambda_3 y} + A_9\, e^{-\lambda_3 y}\right) \end{bmatrix} e^{2iwt} \quad (55)$$

Where;

$$A_0 = \frac{e^{-2iwt}}{e^{-\lambda_4} - e^{\lambda_4}},\ A_1 = -A_0 e^{2\lambda_4}, A_2 = \frac{e^{-2iwt}}{e^{-\lambda_3} - e^{2\lambda_3}}, A_3 = -A_2\, e^{2\lambda_3}, A_4 = \frac{\sigma}{\lambda_1^2}, A_5 = \frac{-f}{(1-\lambda_1^2)},$$

$$A_6 = \frac{(A_4 + A_5 e)\, e^{2\lambda_1} - (A_4 + A_5 e^{-1})}{e^{-\lambda_1} - e^{3\lambda_1}}, A_7 = -A_6 e^{2\lambda_1} - (A_4 + A_5 e)\, e^{\lambda_1}, A_8 = \frac{-dloA_3}{\lambda_3^2 - \lambda_4^2}$$

$$A_9 = \frac{-dLoA_2}{\lambda_3^2 - \lambda_4^2}, A_{10} = -\frac{(A_8 e^{-\lambda_3} + A_9\, e^{-\lambda_3}) + (A_8 e^{\lambda_3} + A_9\, e^{-\lambda_3})e^{-2\lambda 4})}{e^{\lambda 4} - e^{-3\lambda_3 4}}$$

$$A_{11} = A_{10}e^{-2\lambda 4} - (A_8 e^{\lambda_3} + A_9\, e^{-\lambda_3})\, e^{-2\lambda 4})e^{-\lambda 4}, A_{12} = \frac{-bA_7}{\beta\,(\lambda_1^2 - \lambda_2^2)}, A_{13} = -\frac{bA_6}{\beta\,(\lambda_1^2 - \lambda_2^2)}$$

$$A_{14} = \frac{-bA_5}{\beta(1 - \lambda_2^2)}, A_{15} = \frac{bA_4}{\beta\lambda_2^2},$$

$$A_{16} = \frac{-(A_{12}\,e^{\lambda_1} + A_{13}\,e^{-\lambda_1} + A_{14}\,e^{-1} + A_{15}) + (A_{12}\,e^{-\lambda_1} + A_{13}\,e^{\lambda_1} + A_{14}\,e + A_{15})e^{2\lambda_2}}{-e^{3\lambda_2} + e^{-\lambda_2}}$$

$$A_{17} = (A_{16}\,e^{2\lambda_2} - A_{12}\,e^{-\lambda_1} + A_{13}\,e^{\lambda_1} + A_{13}\,e + A_{15}))e^{\lambda_2}$$

$$A_{18} = -\frac{A_3\,e^{iwt}}{\lambda_3^2 - \lambda_1^2}, A_{19} = -\frac{A_2\,e^{iwt}}{\lambda_3^2 - \lambda_1^2}, A_{20} = -\frac{e^{iwt}}{\lambda_1^2}$$

$$A_{21} = \frac{-(A_{18}e^{-\lambda_3} - A_{19}e^{\lambda_3} + A_{20}) + (A_{18}e^{\lambda_3} - A_{19}e^{-\lambda_3} + A_{20})e^{-2\lambda_1}}{e^{\lambda_1} - e^{-3\lambda_1}}$$

$$A_{22} = A_{21}e^{-2\lambda_1} - (A_{18}e^{\lambda_3} + A_{19})e^{-\lambda_3} + A_{20})e^{-\lambda_1}, A_{23} = \frac{-B_2 dA_1}{(\lambda_4^2 - \lambda_3^2)}, A_{24} = \frac{-B_2 dA_0}{(\lambda_4^2 - \lambda_3^2)}$$

$$A_{25} = \frac{-E_c d\lambda_1^2 A_7^2}{(4\lambda_1^2 - \lambda_3^2)}, A_{26} = \frac{2dE_c\lambda_1 A_5 A_7}{((\lambda_1 - 1)^2 - \lambda_3^2)}, A_{27} = \frac{-2dE_c\lambda_1 A_5 A_6}{((-\lambda_1 - 1)^2 - \lambda_3^2)}, A_{28} = \frac{-E_c d\lambda_1^2 A_6^2}{(4\lambda_1^2 - \lambda_3^2)}, A_{29} = \frac{-E_c dA_5^2}{(4 - \lambda_3^2)}$$

$$A_{30} = \frac{-\left(2dE_c\lambda_1^2 A_6 A_7 - dN_r e^{-2iwt}\right)}{\lambda_3^2}$$

$$A_{31} = \frac{1}{(e^{-\lambda_3} - e^{3\lambda_3})}\Big(\big(A_{23}e^{-\lambda_4} + A_{24}e^{\lambda_4} + A_{25}e^{-2\lambda_1} + A_{26}e^{-(\lambda_1 - 1)} + A_{27}e^{-(-\lambda_1 - 1)} + A_{28}e^{2\lambda_1} + A_{29}e^2 + A_{30}\big)e^{2\lambda_3} - \big(A_{23}e^{\lambda_4} + A_{24}e^{-\lambda_4} + A_{25}e^{2\lambda_1} + A_{26}e^{(\lambda_1 - 1)} + A_{27}e^{(-\lambda_1 - 1)} + A_{28}e^{-2\lambda_1} + A_{29}e^{-2} + A_{30}\big)\Big)$$

$$= A_{32} = -A_{31}e^{2\lambda_3} - \big(A_{23}e^{-\lambda_4} + A_{24}e^{\lambda_4} + A_{25}e^{-2\lambda_1} + A_{26}e^{-(\lambda_1 - 1)} + A_{27}e^{-(-\lambda_1 - 1)} + A_{28}e^{2\lambda_1} + A_{29}e^2 + A_{30}\big)e^{\lambda_3}$$

RESULTS

The effect of Prandtl number (P_r), stoke constant (K), Eckert number (E_c), modified Hartman number (H_r), particle mass parameter (G), temperature relaxation time parameter (L_0), fluid concentration parameter (R), dimensionless stress coefficient per unit volume (β), dimensionless pressure gradient **(α),** Hartman number (H),radiation parameter (N_r), Grashof number (G_r), on the velocity$u(y,t)$ of fluid particle, velocity $u_p(y,t)$ of dusty particle, temperature $\theta(y,t)$of fluid particle and temperature$\theta_p(y,t)$ of dusty particle were presented and analyzed graphicallyusing computer symbolic algebraic package MAPLE 17.

Scientia Africana, Vol. 24 (No. 1), February, 2025. Pp 33-50
© Faculty of Science, University of Port Harcourt, Printed in Nigeria *ISSN 1118 – 1931*

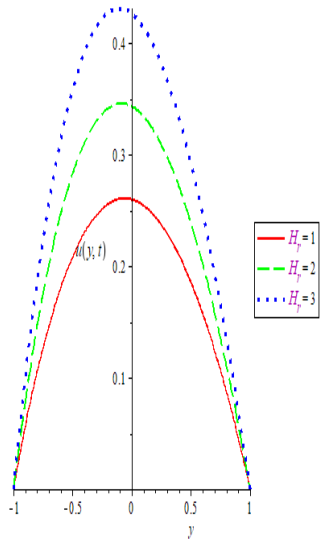

Figure 1: Effect of Modified Hartman Number H_r on V

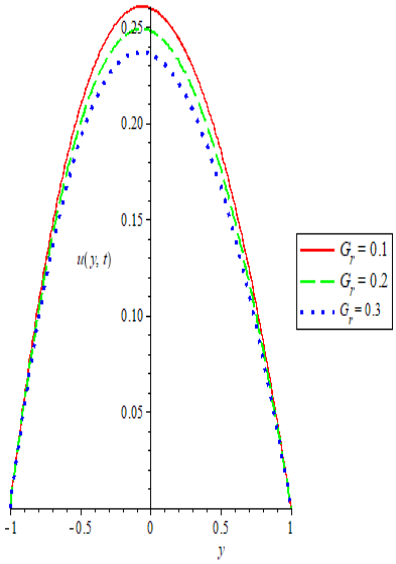

Figure 2: Effect of Grashof Number G_r on Velocity of fluid $u(y,t)$ against Distance y

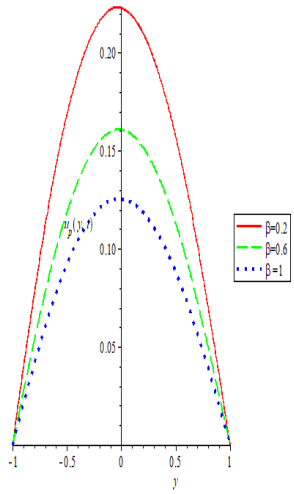

Figure 3: Effect of dimensionless stress coefficient per unit volume (β) on Velocity of fluid $\mathbf{u(y,t)}$ against Distance y

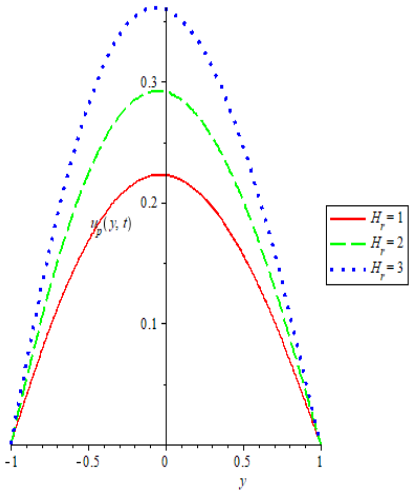

Figure 4: Effect of Modified Hartman Number $\mathbf{H_r}$ on Velocity of dusty particles $\mathbf{u_p(y,t)}$ against Distance y

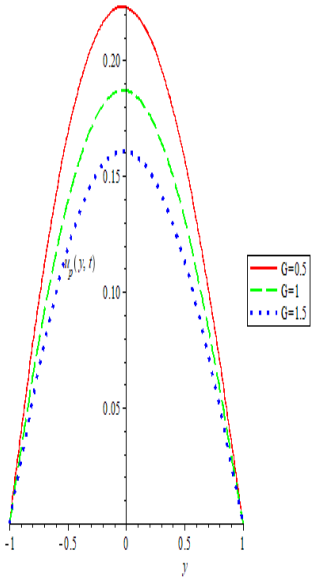

Figure 5: Effect of particle mass parameter (G) on Velocity of dusty particles $u_p(y,t)$ against Distance y

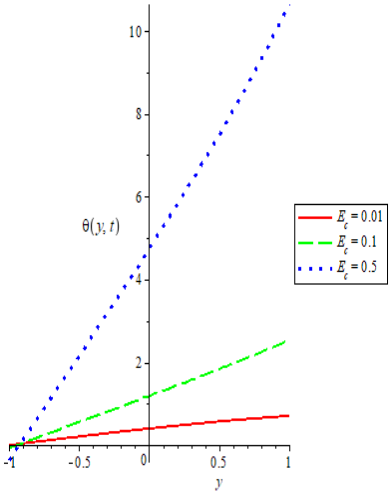

Figure 6: Effect of Eckert number (E_c) on Temperature of fluid $\theta(y,t)$ against Distance y

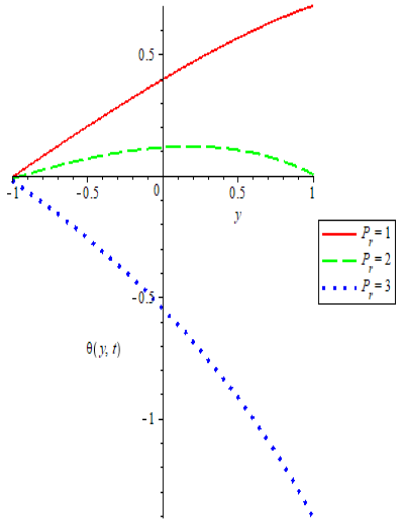

Figure 7: Effect of Prandtl number (P_r) on Temperature of fluid $\theta(y,t)$ against Distance y

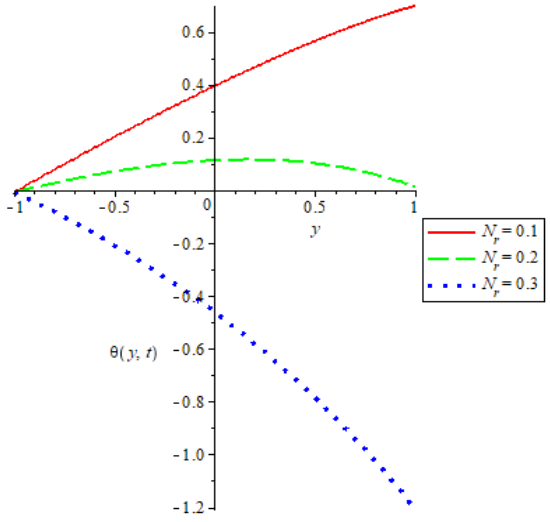

Figure 8: Effect of Radiation parameter (N_r) on Temperature of fluid $\theta(y,t)$ against Distance y

Scientia Africana, Vol. 24 (No. 1), February, 2025. Pp 33-50
© Faculty of Science, University of Port Harcourt, Printed in Nigeria *ISSN 1118 – 1931*

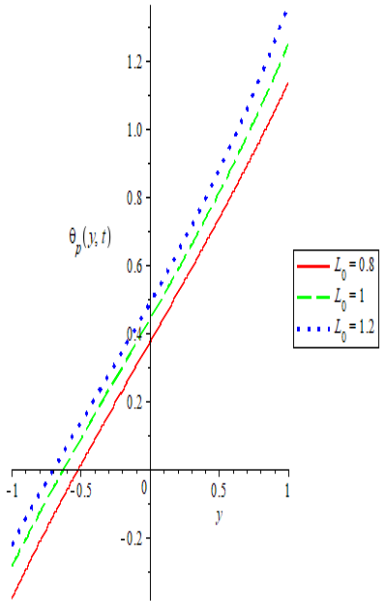

Figure 9: Effect of temperature relaxation time parameter (L_0) on Temperature of dusty particle $\theta(y,t)$ against Distance y

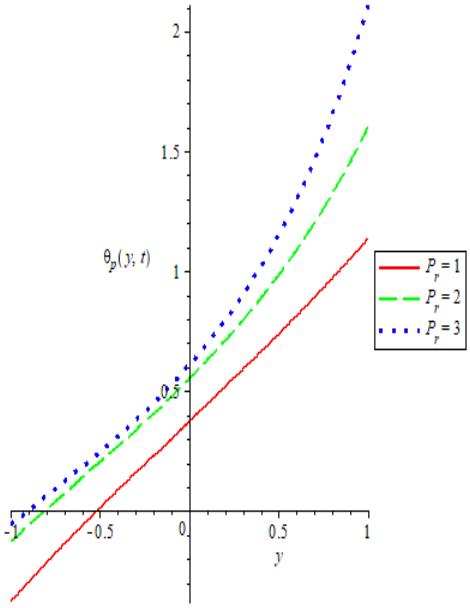

Figure 10: Effect of Prandtl number (P_r) on Temperature of dusty particle $\theta_p(y,t)$ against Distance y

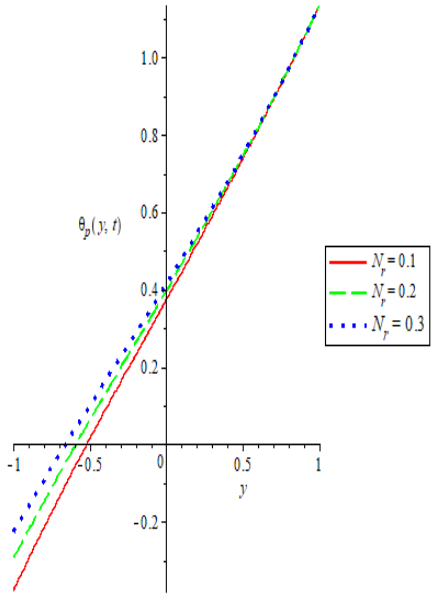

Figure 11: Effect of Radiation parameter (N_r) on Temperature of dusty particles $\theta_p(y,t)$ against Distance y

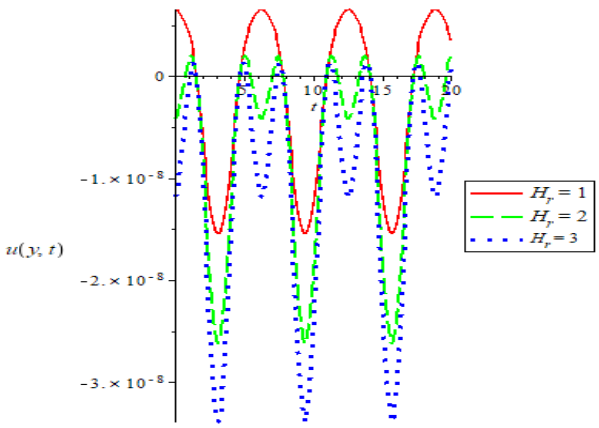

Figure 12: Effect of Modified Hartman Number H_r on Velocity of fluid $u(y,t)$ against time t

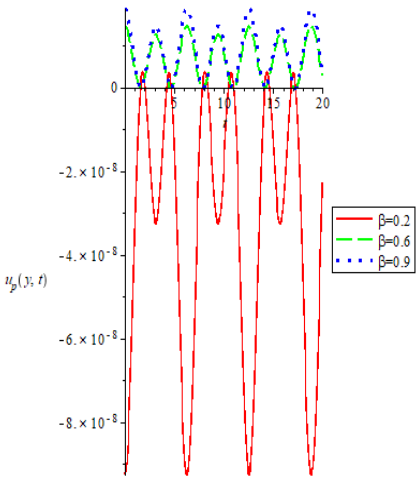

Figure 13: Effect of dimensionless stress coefficient per unit volume (β) on Velocity of fluid $u_p(y,t)$ against time t

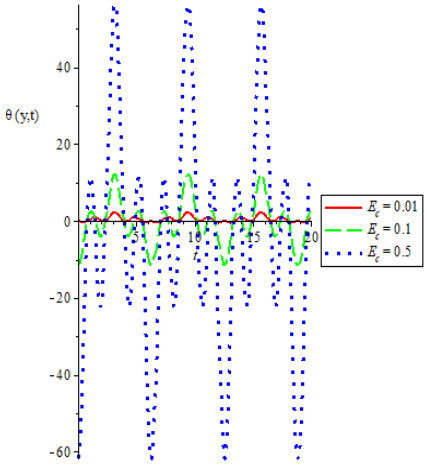

Figure 14: Effect of Eckert number (E_c) on Temperature of fluid $\theta(y,t)$ against time t

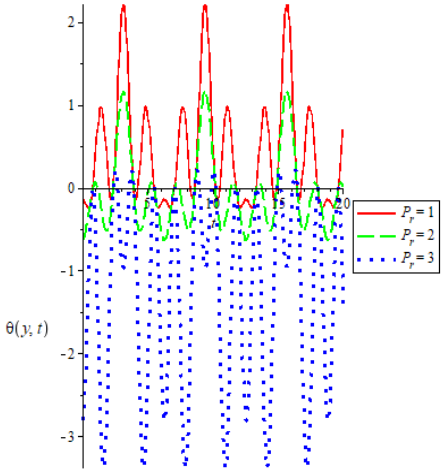

Figure 15: Effect of Prandtl number (P_r) on Temperature of fluid $\theta(y,t)$ against time t

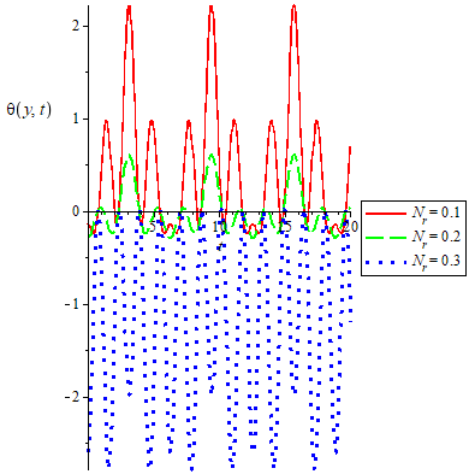

Figure 16: Effect of Radiation parameter (N_r) on Temperature of fluid $\theta(y,t)$ against time t

DISCUSSION OF RESULTS

Figure 1 shows the effect of modified Hartman number H_r on velocity of fluid $u(y,t)$ against distancey. it is observed that velocity of fluid increases to a point and later decreases along distance and this velocity increases as modified Hartman number H_r increases.

Figure 2 shows the effect of Grashof number G_r on velocity of fluid $u(y,t)$ against distance y. it is observed that velocity of fluid increases to a point and later decreases along distance and this velocity decreases as Grashof number G_r increases.

Figure 3 shows the effect of dimensionless stress coefficient per unit volume (β) on velocity of fluid $u(y,t)$ against distance y. it is observed that velocity of fluid increases to a point and later decreases along distance and

Scientia Africana, Vol. 24 (No. 1), February, 2025. Pp 33-50
© Faculty of Science, University of Port Harcourt, Printed in Nigeria *ISSN 1118 – 1931*

this velocity decreases as dimensionless stress coefficient per unit volume (β) increases.

Figure 4 shows the effect of modified Hartman number H_r on velocity of dusty particles $u_p(y,t)$ against distance y. it is observed that velocity of fluid increases to a point and later decreases along distance and this velocity increases as modified Hartman number H_r increases.

Figure 5 shows the effect of particle mass parameter (G) on velocity of dusty particles $u_p(y,t)$ against distance y. it is observed that velocity of fluid increases to a point and later decreases along distance and this velocity decreases as particle mass parameter (G) increases.

Figure 6 shows the effect of Eckert number (E_c) on temperature of fluid $\theta(y,t)$ against distance y. it is observed that temperature of fluid increases along distance and this temperature increases as Eckert number (E_c) increases.

Figure 7 shows the effect of Prandtl number (P_r) on temperature of fluid $\theta(y,t)$ against distance y. it is observed that temperature of fluid decreases along distance and this temperature decreases as Prandtl number (P_r) increases.

Figure 8 shows the effect of radiation parameter (N_r) on temperature of fluid $\theta(y,t)$ against distance y.it is observed that temperature of fluid decreases along distance and this temperature decreases as radiation parameter (N_r) increases.

Figure 9 shows the effect of temperature relaxation time parameter (L_0) on temperature of dusty particle $\theta_p(y,t)$ against distance y. it is observed that temperature of dusty particle increases along distance and this temperature increases as temperature relaxation time parameter (L_0) increases.

Figure 10 shows the effect of Prandtl number (P_r) on temperature of dusty particle $\theta_p(y,t)$ against distance y.it is observed it is observed that temperature of dusty particle increases along distance and this temperature increases as Prandtl number (P_r) increases.

Figure 11shows the effect of radiation parameter (N_r) on temperature of dusty particles $\theta_p(y,t)$ against distance y. it is observed that temperature of dusty particle increases along distance and this temperature increases and later converges at a point as radiation parameter (N_r) increases.

Figure 12 shows the effect of modified Hartman number H_r on velocity of fluid $u(y,t)$ against time t. it is observed that velocity of fluid moves in a sinusoidal way against time and this velocity increases as modified Hartman number H_r increases.

Figure 13 shows the effect of dimensionless stress coefficient per unit volume (β) on velocity of fluid $u_p(y,t)$ against time t. it is observed that velocity of dusty particles moves in a sinusoidal way against time and this velocity increases as dimensionless stress coefficient per unit volume (β) increases.

Figure 14 shows the effect of Eckert number (E_c) on temperature of fluid $\theta(y,t)$ against time t. it is observed that temperature of fluid moves in a sinusoidal way against time and this temperature increases as Eckert number (E_c) increases.

Figure 15 shows the effect of Prandtl number (P_r) on temperature of fluid $\theta(y,t)$ against time t. it is observed that temperature of fluid moves in a sinusoidal way against time and this temperature decreases as Prandtl number (P_r) increases.

Figure 16 shows the effect of radiation parameter (N_r) on temperature of fluid $\theta(y,t)$ against time t. it is observed that temperature of fluid moves in a sinusoidal way against time and this temperature decreases as radiation parameter (N_r) increases.

CONCLUSION

This mathematical analysis investigates the heat transfer characteristics of MHD dusty fluid flow between two Riga plates embedded in a porous medium. The non-

dimensionalization of model equations revealed significant insights into the effects of various dimensionless parameters on fluid velocity and temperature.

Key Findings:

At the end of this analysis, several insightful key observations were made. These includes:

1. The Modified Hartman number (H_r) enhances fluid and dusty particle velocities, indicating the significance of magnetic field strength in MHD flows.
2. Grashof number (G_r) and dimensionless stress coefficient per unit volume (β) decrease fluid velocity, highlighting the opposing effects of buoyancy and particle interactions.
3. Particle mass parameter (G) reduces dusty particle velocity, demonstrating the impact of particle inertia on flow behavior.
4. Eckert number (E_c) increases fluid temperature, illustrating the role of viscous dissipation in heat transfer.
5. Prandtl number (P_r) and radiation parameter (N_r) decrease fluid temperature, emphasizing the combined effects of thermal diffusivity and radiative heat transfer.
6. Temperature relaxation time parameter (L_0) increases temperature, indicating the significance of thermal relaxation in heat transfer processes.
7. Radiation parameter (N_r) also increases dusty particle temperature, underscoring the importance of radiative effects in particle heating.

The analysis of MHD dusty fluid flow between Riga plates embedded in a porous medium has broad applications across various fields. By improving knowledge of fluid flow and heat transfer under magnetic fields, it helps energy systems optimise operations in nuclear fusion reactors, MHD pumps, and geothermal energy systems. It facilitates the design of effective dust control, combustion chamber, and multiphase oil recovery systems in industrial operations. It supports pollution control and climate research by predicting the movement and dispersion of particle contaminants in porous medium through environmental modelling.

Enhancing targeted medication delivery systems and comprehending blood flow dynamics in magnetic fields are examples of biomedical applications. This analysis is useful for optimising fluid flow, heat transfer, and particle behaviour across a variety of scientific and engineering applications. Furthermore, the understanding of heat transfer mechanisms is essential for spacecraft thermal systems, heat exchangers, and materials intended for thermal insulation.

REFERENCES

Ahmad, A. (2019): Flow Control of Non-Newtonain Fluid using Riga Plate:Reiner-Phillipoff and Powell-Eyring Viscosity Models. *Journal of Applied Fluid Mechanics, Vol. 12, No. 1, pp. 127-133.*

Alfvén, H. (1942): Existence of electromagnetic-hydrodynamic wavesNature, *150 (3805), pp. 405-406*

Anjum, A., Mir,N.A., Farooq, M., Khan,M. I. and Hayat, T. (2018): Influence of thermal stratification and slip conditions on stagnation point flow towards variable thicked Riga plate. *Results in Physics. Vol.9,pp.1021-1030.*

Chiam, T. C. (1995): Hydromagnetic flow over a surface stretching with a power-law velocity*International Journal of Engineering Science, vol. 33, no. 3, pp. 429-435.*

Cogley, A. C. L., Vinvent, W. C. and Gilees, S. E. (1968): Differential approximation for radiative transfer in a non-grey gas near equilibrium. *American Institute of Aeronautics and Astronautics. 551.*

Ferraro, V.C.A. and Plumpton, C. (1966): An Introduction to Magneto Fluid Mechanics. *Clarandon Press, Oxford.*

Hayat, T., Abbas T., Ayub, M., Faroq,M. and Alsaedi, A.(2016): Flow of nanofluid due

Scientia Africana, Vol. 24 (No. 1), February, 2025. Pp 33-50
© Faculty of Science, University of Port Harcourt, Printed in Nigeria *ISSN 1118 – 1931*

to convectively heated Riga plate with variable thickness. *Vol.222,pp.854-862.*

Iqbal Z., Azhar E., Mehmood Z and Maraj E.N. (2017): Melting heat transport of nanofluidic problem over a Riga plate with erratic thickness: Use of Keller Box scheme, *Results in Physics, vol.7, pp.3648–3658.*

Iqbal, Z., Azhar, E., Mehmood, Z. and Maraj, E.N. (2018): Unique outcomes of internal heat generation and thermal deposition on the viscous dissipative transport of viscoplastic fluid over a Riga plate. *Communications in Theoretical Physics,Vol.69, pp. 68-76.*

Islam,M. R. and Nasrin,S. (2020): Dusty Fluid Flow Past between Two Parallel Riga Plates Embedded in a Porous Medium. *International Journal of Advances in Applied Mathematics and Mechanics, Vol 8(2) ,1 – 14, 2347-2529.*

Islam,M. R. and Nasrin,S. (2021): Unsteady Couette Flow of Dusty Fluid Past between Two Riga Plates. *European Journal of Scientific Research Vol. 159 (2) pp.18 – 32*

Jimoh, O. R and Abdullahi, D. (2023): Effect of Heat and Mass Transfer on Magneto-Hydrodynamic Flow with Chemical Reaction and Viscous Energy Dissipation Past an Inclined Porous Plate. *Scientia Africana, Vol. 22 (No. 2). Pp 259-276*

Jimoh, O. R. and Ibrahim, I. (2023): Effect of Viscous Energy Dissipation on Transient Laminar Free Convective Flow of a Dusty Viscous Fluid through a Porous Medium. *Journal of Applied Sciences & Environmental Management Vol. 27 (9) 1925-1935*

Kalpana, G. and Saleem, S. (2022): Heat Transfer of Magnetohydrodynamic Stratified Dusty Fluid Flow through an Inclined Irregular Porous Channel. *Nanomaterials vol 12(19): 3309.*

Kataria, H. R. and Patel,H. R.(2016):Soret and heat generation eff ects on MHD Casson fluid flow past an oscillating vertical plate embeddedthrough porous medium. *Alexandria Engineering Journal 55(3)*

Kumar, R. (2014): Unsteady Flow of a Dusty Conducting Fluid between Parallel Porous Plates through Porous Medium with Temperature Dependent Viscosity.*International Journal of Engineering & Technical Research, ISSN: 2321-0869.*

Maher,M.M., Mekheimer,K. S., Al-Wahsh,H. and Zaher,A.Z. (2024): Hydrodynamic Impact of Dusty Fluid-Suspended Solid Particles in a Single-Walled Corrugated Channel for Water-Curing Infrastructure Networks.*Chinese Journal of Physics08.014*

Mehta, T., Mehta, R. and Mehta, A. (2020): Oscillatory Fluid Flow and Heat Transfer Through Porous Medium Between Parallel Plates with Inclined Magnetic Field, Radiative Heat Flux and Heat Source, *International Journal of Applied Mechanics and Engineering, vol.25, No.2, pp.88-102.*

Pai, S.I. (1962):*Magnetogasdynamics and Plasma Dynamics.*Springer Verlag, Berlin.

Seddeek, M.A. and Salem, A.M. (2005): Laminar Mixed Convection Adjacent to Vertical Continuously Stretching Sheets with Variable Viscosity and Thermal Diffusivity, Heat and Mass Transfer, *41, 1048-1055.*

Yabo, I. B., Kumar, B. J. and Jeng-Eng, L. (2018): Couette Flow of Conducting Fluid. *International Journal of Theoretical and Applied Mathematics, Vol.4(1), pp. 8-21.*